# CRACK TRAPPING AND BRIDGING AS TOUGHENING MECHANISMS IN HIGH STRENGTH CONCRETE

VICTOR C. LI
The University of Michigan, Ann Arbor, MI 48109-2125, U.S.A.
and
J. HUANG
The Massachusetts Institute of Technology, Cambridge, MA 02139, U.S.A.

## ABSTRACT

This paper discusses the likely sources of fracture toughness in high strength concrete. These sources include the crack front trapping mechanism and the crack flank bridging mechanism resulting from interaction between the cement matrix and well bonded aggregates. The magnitude of toughness provided by each type of mechanisms are estimated.

## INTRODUCTION

High strength concrete behaves quite differently from normal strength concrete. It has a stronger (higher strength, higher stiffness) and tougher (higher fracture toughness) cement paste due to a lower water/cement ratio, which results in a closer packing of cement grains with reduced amount of pores and crack like flaws. Apart from the microstructurally improved matrix, high strength concrete also has a stronger interface between the cement matrix and the aggregates, presumably resulting from reduction of excess bleeding and the filling in of gaps by the commonly used silica fume in this material. These microstructural differences between high strength concrete and normal strength concrete lead to significant differences in the deformation and fracture behavior. For example, it is well known that high strength concrete tend to behave more linear elastically up to the peak strength, whereas normal strength concrete typically exhibit non-linear behavior plausibly due to interfacial crack expansion [e.g. 1, 2, 3] prior to peak strength. Further, fracture development in high strength concrete is usually accompanied by a relatively small process zone and tends to be better described by linear elastic fracture mechanics in comparison to normal strength concrete [e.g. 4]. When the fracture surface is examined, high strength concrete typically shows a smooth and flat surface with fractured aggregates. In contrast, normal strength concrete

fracture surface are usually tortuous and exhibits evidence of aggregate pull-out [e.g. 2,5,6].

In normal strength concrete, it is generally accepted that much of the composite fracture toughness comes from the cement/matrix interfacial cracking and aggregate bridging mechanism in an extensive process zone at a macroscopic crack tip [e.g. 7]. These energy absorption mechanisms are likely to be significantly reduced in high strength concrete. Yet, most measurement of fracture toughness indicate that high strength concrete maintains the same toughness as in normal strength concrete, and in some instances even a positive correlation between toughness and strength [e.g. 4, 6, 8, 9]. However, it should be pointed out that this increase, if at all, of fracture toughness is usually at a lower rate than the increase in tensile strength, and therefore results in a material with limited post-crack ductility or a drop in the material characteristic length $l_{ch}$ [10]. This paper attempts to address the source of toughening mechanisms in high strength concrete, the understanding of which may lead to systematic engineering of its microstructures towards improvement of its post-crack ductility, without losing its advantageous strength characteristics.

## THE CRACK FRONT TRAPPING MECHANISM

The crack front trapping mechanism was first suggested by Lange [11,12] based on observations of crack front bowing between $Al_2O_3$ particles in a sodium borosilicate glass. The essential idea is that a straight crack front approaching a well bonded particle would be hindered in its propagation at the particle site (Figure 1). As the rest of the crack front bows around this trap site, the stress intensity factor at this bow out portion of the crack front is reduced resulting in a retardation of its propagation process. (The stress intensity factor of the crack front at the trap site, however, would rise with increasing amount of bowing of the adjacent crack front.) Further propagation would require additional loading, thus providing an apparent toughening effect to the composite.

The presence and effectiveness of the crack front trapping mechanism depends on a number of features of the material structure. If the particle is weak, its tensile strength or fracture toughness may be exhausted by the presence of the high tensile stress and stress intensity factor of the impinging crack front, and the trap site would then be eliminated by particle failure. If the matrix/particle interface is weak, the crack front at the trap site may rapidly turn onto an interfacial crack, and the trap site is again lost.

It is a general practice to use higher quality aggregates of smaller sizes (compared to that used in normal strength concrete) in high strength concrete. Together with an improved interfacial bond, high strength concrete probably provides a material structure favorable to the presence of the crack trapping mechanism. The smaller size aggregates would create larger number of trap sites for a given volume fraction. Although the trapping mechanism has not be directly observed experimentally, the conditions of its presence discussed above and rough estimates of the level of toughening to be presented below suggest that its presence may not be unreasonable. Further direct observations would be needed for confirmation.

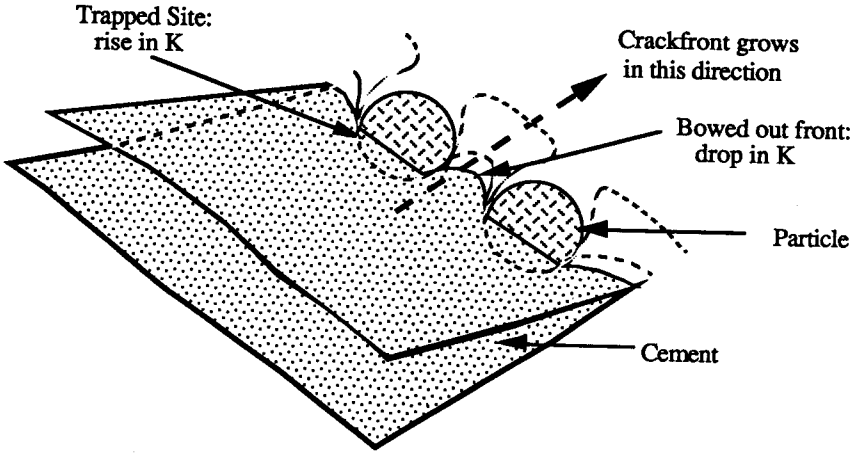


Figure 1. Stages of crack front motions, with portions of crack front being trapped by well bonded particles

## THE CRACK BRIDGING MECHANISM

If the crack front passes the trap site without rupturing the particle or the interfacial bond, then a complete bridge is left behind. This particle bridge acts as a spring exerting a closing pressure on the crack flanks. The resulting reduction of the crack driving force leads to an additional toughening effect. This crack bridging toughening mechanism has been studied by Krstic [13], Rose [14, 15] and Budiansky et al [16] for particulate reinforced ceramics.

As the crack front moves forward, a series of bridges will be left behind forming a process zone (Figure 2). The extent of the process zone and the amount of energy absorbed depends on the constitutive behavior of the bridge 'springs'. Figure 3 illustrates schematically the crack tip-process zone (smeared out) stress field for several possible scenarios relating to the bridging mechanism. If the particles are well-bonded and behaves elastic-plastically (Figure 3a), as in Al particle reinforced glass [e.g. 16], process zone energy absorption could be significant. If the particles debond frictionally in the process zone, they may be regarded as rigid-softening as illustrated in Figure 3b. This is likely to be the case for

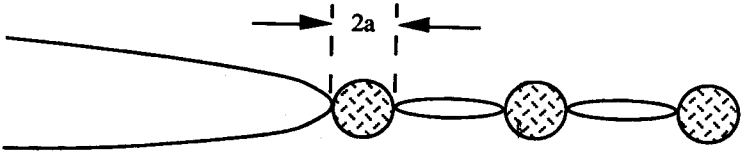


Figure 2. Process zone with particles bridging crack flanks

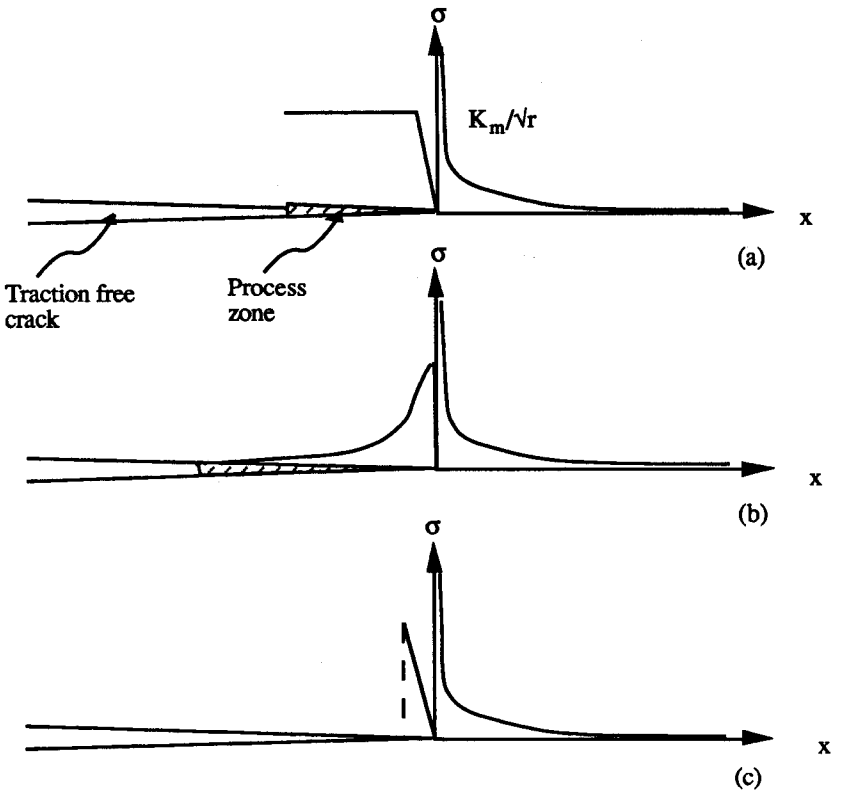


Figure 3. Schematics of crack tip stress field with bridging particles in process zone behaving (a) elastic plastically, (b) rigid softening, and (c) elastic brittlely

normal strength concrete, although the bridges left behind the crack front may not be intact to start with (i.e. the trapping mechanism may be incomplete). If the particles behave elastic-brittlely (Figure 3c), the energy absorption in the process zone, which length may be expected to be small, would not be significant. This is likely to be the case of high strength concrete in which the aggregates would be elastically stretched and eventually ruptured in the small process zone.

## TOUGHENING RATIOS OF PARTICULATE REINFORCED COMPOSITES

In order to consider the approximate effects of crack front trapping and crack flank bridging on composite toughening at steady state, (steady state here means that the process zone has reached a fixed size and simply translates as the physical crack extends), it will be convenient to consider the crack tip region, including the process zone, to be contained in a far field K-dominant region. Following [14, 16, 17], and expressing the path-independent property of

the J-integral [19] for the closed contour shown in Figure 4, the three contributions of the J-integral are:

$$J_\infty + J_b + J_{tip} = 0 \tag{1}$$

The $J_\infty$ term represents the far field applied load and contains information on the structural geometry. The $J_{tip}$ is the critical J value for advancing the crack front against the composite toughness which includes the effect of trapping but not bridging. Finally $J_b$ is the energy consumed by the extended springs in the process zone. Thus in terms of energetics, (1) implies that the energy release rate associated with far field

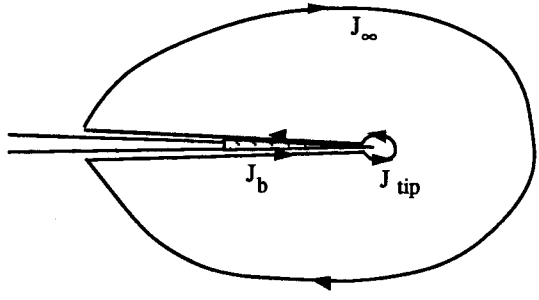


Fig. 4: J-integral contour around fracture process zone and crack tip

loading is absorbed by the creation of unit composite fracture surface, as well as by the spring deforming process. Evaluating the three J-terms, (1) becomes

$$\frac{K^2(1-\upsilon^2)}{E} = \frac{\lambda^2 K_m^2(1-\upsilon^2)}{E} + \int_0^{\delta^*} \sigma_b(\delta)\, d\delta \tag{2}$$

where E and $\nu$ are the composite Young's Modulus and the Poisson's ratio, $K_m$ is the matrix toughness, and $\delta^*$ is the critical opening at which the bridging spring loses all load carrying capacity. Clearly the integral term in (2) is just the area under the spring constitutive law. The factor $\lambda$ in the first term of the right hand side represents the toughening ratio due to the crack front trapping mechanism described above, and which shall be determined.

When the trapping effect is ignored, i.e. setting $\lambda = 1$, equation (2) may be regarded as a generalization of the now familiar fracture criteria of Irwin [19], Barenblatt [20] and Dugdale [21] for monolithic materials. Equation (2) reduces to Irwin's fracture criterion if the bridging zone does not exist, so that fracture propagation is resisted by the matrix toughness $K_m$ only. If, on the other hand, $K_m$ is negligible compared to the bridging term, as in the case of certain fiber reinforced composites with low toughness matrix, then equation (2) reduces to a form similar to the fracture criterion expressed by Barenblatt. Finally, if again, $K_m$ is negligible, and that $\sigma_b$ is a constant independent of $\delta$, then Dugdale's fracture criterion will result.

Rice [22] analyzed the toughening effect of crack front trapping by an array of periodically placed square cross-sectioned impenetrable particles which have the same elastic moduli as the matrix material. For simplicity we assume that the crack front between particles can attain a semicircular shape prior to breaking off (i.e. re-forming a straight crack front and passing the trap site), analogous to that expected by the line tension theory in dislocation bowing between pinned ends, so that the maximum amount of crack front penetration between particles is equal to half the edge to edge distance between adjacent particles. Under these conditions, the maximum attainable toughening ratio $\lambda$ of Rice[22] may be rewritten in terms of the volume fraction of particles:

$$\lambda = \left\{ 1 - \frac{(\pi/4)(1-V_f)}{\ln\left[\frac{1+\cos(\pi V_f/2)}{\sin(\pi V_f/2)}\right]} \right\}^{-1} \tag{5}$$

Equation (5) for the toughening ratio is based on an asymptotic analysis for which crack bowing causes the crack front to be slightly deviated from a straight line. This implies that (5) will not be accurate for very dilute concentrations of particles in the composite. Fares [23] reanalyzed this problem numerically for a cosine shape crack front and found that the asymptotic solution is valid for particle concentrations in excess of 0.2. For volume fractions of 0.3, 0.5 and 0.7, the toughening ratio based on (5) will be 1.63, 1.80 and 1.93 respectively.

We are now in a position to evaluate (3), using (4) and (5), for the combined toughening effect of trapping and bridging in high strength concrete. For the range of parametric values mentioned earlier, the combined toughening ratio $K_{eff}/K_m$ will be 1.89, 1.99 and 2.01 for $V_f$ =0.3, 0.5, and 0.7 respectively. For a=20mm, S=20 MPa, $K_{eff}/K_m$ will be 3.18, 3.00 and 2.53. It is interesting to note (see also (4)) that there is a maxima in the toughening ratio which shifts towards the low volume fraction end for high aggregate strength and/or large aggregate size, and vise versa.

## COMPARISONS WITH AVAILABLE EXPERIMENTAL DATA

There is not much experimental fracture toughness data of high strength concrete. Tognon and Cangiano [6] measured the fracture toughness of a high strength concrete ($f_c$ = 85-120 MPa, maximum aggregate size of 20mm) with a water cement ratio of 0.33 and found that the composite $K_{Ic}$ = 1.0-1.5 MPa $\sqrt{m}$. The toughness of the cement matrix is not reported. However, Higgins and Bailey [24] made toughness measurements of cement paste of various water/cement ratio and curing time. These data are summarized in Figure 5. The 28 day toughness for a w/c ratio of 0.33 cement would be approximately equal to 0.4 MPa $\sqrt{m}$.

Our objective is to evaluate the composite toughening ratio $K/K_m$ which accounts for both trapping and bridging. This may be obtained from (2), as:

$$\frac{K_{eff}}{K_m} = \sqrt{\left[\lambda^2 + \frac{E \cdot \int_0^{\delta^*} \sigma_b(\delta)\, d\delta}{(1-\upsilon^2)\cdot K_m^2}\right]} \tag{3}$$

where the far field K assumes the effective composite toughness $K_{eff}$ when the fracture condition for small scale yielding is met.

## ESTIMATION OF TOUGHENING DUE TO BRIDGING AND TRAPPING IN HIGH STRENGTH CONCRETE

To evaluate the integral term in (3), it is necessary to assume certain constitutive relation for the spring action in the bridging zone. For high strength concrete, a reasonable assumption would be a linear elastic behavior up to aggregate fracture. Under this condition, an approximate expression has been derived by Budiansky et al [16] for the integral term:

$$\int_0^{\delta^*} \sigma_b(\delta) d\delta = \frac{\pi}{2} \frac{S^2 a V_f (1-\sqrt{V_f})(1-V_f)(1-\upsilon_m^2)}{E_m} \tag{4}$$

where S is the aggregate tensile strength, a is the (here assumed) average diameter of aggregates (assumed spherical in shape), $V_f$ the volume fraction of aggregates, and $\nu_m$ and $E_m$ are the cement matrix Poisson's ratio and Young's Modulus. For a typical high strength concrete, it may be reasonable to assume a = 10 mm, S = 10 MPa, $K_m$= 0.4 MPa $\sqrt{m}$, and further assuming that the elastic properties of the cement matrix are not significantly different from that of the composite. The toughening ratio due to bridging may then be obtained from (3) and (4), setting $\lambda = 1$, and found to be 1.39, 1.31, and 1.16, corresponding to volume fractions of 0.3, 0.5, and 0.7 respectively. These estimates should, however, be interpreted with caution because of the idealized assumptions built into (4), and because high strength concrete typically employs both fine and coarse aggregates with a range of size distributions and usually not spherically in shape.

If (4) represents a fair description of toughening by bridging, then it appears that the tensile strength of aggregates would be important in controlling composite toughness, and this is also consistent with experience in controlling compressive strength. However, (4) also suggests that larger size aggregates would be beneficial to composite toughness, whereas most empirical studies seem to indicate the need of small aggregates for good compressive strength performance. To maintain both strength and toughness, it may be necessary to optimize the mix with respect to aggregate size.

Thus the toughening ratio for this high strength concrete is roughly 2.5 to 3.75.

In another series of fracture experiment of high strength concrete (w/c = 0.25; 14 day compressive strength of 85MPa, maximum aggregate size of 9.5mm) performed by Gettu et al [4], the fracture toughness based on infinite size (from extrapolation) specimen was found to be 0.95 MPa$\sqrt{m}$. With the cement toughness again assumed to be 0.4 MPa$\sqrt{m}$ (rough estimate from Figure 5 for w/c = 0.25 and curing age of 14 days), the toughening ratio for this high strength concrete is approximately equal to 2.38.

The theoretically calculated range of toughening ratio for high strength concrete is not incompatible to the measured values described above, given the approximations made in the theoretical estimates, uncertain parametric values, and experimental data scatter.

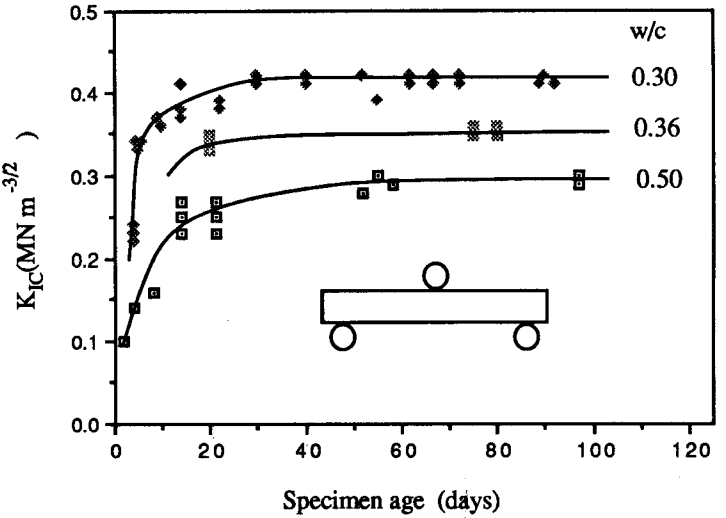


Figure 5. Fracture toughness of cement of different w/c ratio and curing age, after [24]

## CONCLUSIONS

It is hypothesized that high strength concrete derives its toughness from a combination of sources involving the crack front trapping mechanism and the crack frank bridging mechanism, in addition to a higher cement matrix toughness due to a reduction in water/cement ratio. These mechanisms were evaluated using theoretical results [16, 22] of toughening ratios for elastic-brittle particulate composites. The theoretically determined toughening ratios were found to be consistent with those from two separate series of experiments [4,6] on the fracture behavior of high strength concrete. The elucidation of the controlling mechanisms suggest possibilities of materials engineering at the micro and meso level in order to overcome certain shortcomings in the properties of high strength concrete.

## REFERENCES


1. ACI Committee 363, State of the art report on high strength concrete, ACI J., 81, 4, 1984, 364-411.

2. Carrasquillo, R.L., Nilson, A.H., and Slate, F.O., Properties of high strength concrete subject to short-term loads, *ACI J.*, May-June 1981, 171-178.

3. Huang, J. and Li, V.C., A meso-mechanical model of the tensile behavior of concrete -- Part I: modelling of pre-peak stress-strain relation", *Composites*, 20, 4, 1989, 361-369.

4. Gettu, R., Bazant, Z.P., and Karr, M.E., Fracture properties and brittleness of high strength concrete, submitted to the *ACI J. of Materials*, 1990.

5. Carrasquillo, R.L., Slate, F.O., and Nilson, A.H., Microcracking and behavior of high strength concrete subject to short-term loading, *ACI J.*, May-June 1981, 179-186.

6. Tognon, G., and Cangiano, S., Fracture behavior of high strength and very high strength concretes, in *International Workshop on Fracture Toughness and Fracture Energy -- Test Methods for Concrete and Rock*, ed. Mihashi, 1988, 77-89.

7. Hillerborg, A., Analysis of one single crack, in Fracture Mechanics of Concrete, ed. F.H. Wittmann, Elsevier, 1983, pp. 223-250.

8. Nallathambi, P., and Karihaloo, B.L., Influence of slow crack growth on the fracture toughness of plain concrete, In *Fracture Toughness and Fracture Energy of Concrete*, F.H. Wittmann, ed., Elsevier Science Publishers, The Netherlands, 1986, 271-280.

9. John, R., and Shah, S.P., Fracture mechanics analysis of high strength concrete, *J. of Materials in Civil Engineering*, 1, 4, 1989, 185-197.

10. Hillerborg, Fracture Mechanics and the concrete codes, in Fracture Mechanics: Application to Concrete, ed. Li, V.C. and Bazant, Z.P., ACI SP-118, 1989, pp.157-170.

11. Lange, F. F., The interaction of a crack front with a second-phase dispersion, *Phil. Mag.*, 22, 1970, 983-992.

12. Lange, F. F., Fracture energy and strength behavior of a sodium borosilicate glass-$Al_2O_3$ composite system, *J. Ceramic Soc. Amer.*, 54, 12, 1971, 614-620.

13. Krstic, V. D., On the fracture of brittle-matrix/ductile-particle composites, *Phil. Mag. A*, 48, 5, 1983, 695-708.

14. Rose, L. R. F., Crack reinforcement by distributed springs, *J. Mech. Phys. Solid*, 35, 4, 1987, 383-405.

15. Rose, L.R.F., Toughening due to crack front interaction with a second phase dispersion, *Mech. of Mat.*, 6, 1987, 11-15.

16. Budiansky, B., Amazigo, J. C. and Evans, A. G., Small-scale crack bridging and the fracture toughness of particulate-reinforced ceramics, *J. Mech. Phys. Solids*, 36, 1988, 167.

17. Marshall, D., and Evans, A.G., The influence of residual stress on the toughness of reinforced brittle materials, *Material Forum*, 11, 1988, 304-312.

18. Rice, J.R., Mathematical analysis in the mechanics of fracture, in *Fracture: An Advanced Treatise*, 2, Academic Press, 1968, pp. 191-311.

19. Irwin, G.R., Analysis of stresses and strains near the end of a crack traversing a plate, *J. Applied Mechanics*, 24 (1957), 361-364.

20. Barenblatt, G.I., Mathematical Theory of Equilibrium Cracks in Brittle Fracture, in: *Advances in Applied Mechanics, VII*, Academic Press, New York, 1962.

21. Dugdale, D.S., Yielding of steel sheets containing slits, *J. Mecha. and Phys. of Solids*, 8, 1960.

22. Rice, J.R., Crack fronts trapped by arrays of obstacles: solutions based on linear perturbation theory, in *Analytical, Numerical and Experimental Aspects of Three Dimensional Fracture Processes*, Ed. Rosakis, A.J., Ravi-Chandar,K., and Rajapakse,Y., AMD-91, ASME, 1988, pp. 175-184.

23. Fares, N., Crack fronts trapped by arrays of obstacles: Numerical solutions based on surface integral representation, J. Appl. Mech., 56, 837-843, Dec., 1989.

24. Higgens, D.D. and Bailey, J.E., Fracture measurements on cement paste, *J. Materi. Sci.*, 11, 1976, 1995-2003.